

Engineering Notes

ENGINEERING NOTES are short manuscripts describing new developments or important results of a preliminary nature. These Notes cannot exceed 6 manuscript pages and 3 figures; a page of text may be substituted for a figure and vice versa. After informal review by the editors, they may be published within a few months of the date of receipt. Style requirements are the same as for regular contributions (see inside back cover).

Effects of Scaled Heatshield Tile Misalignment on Orbiter Boundary-Layer Transition

W.D. Goodrich*

NASA, Houston, Texas

and

C.J. Stalmach Jr.†

Vought Corporation, Dallas, Texas

Introduction

THE objective of this study was to develop a capability for assessing the sensitivity of the orbiter windward surface heat-transfer rate and boundary-layer transition data to surface features, or "roughness elements," characteristic of randomly misaligned heatshield tiles. To this end, selected tiles were precisely formed on the surface of a 0.0175-scale orbiter model using both selective electroless plating^{1,2} and selective electrochemical etching techniques. Wind-tunnel results indicated that the effects of roughness on the location of boundary-layer transition for the orbiter was greatly influenced by the temperature ratio T_w/T_f .

Model Development Program

The pattern and geometry used for simulating misaligned heatshield tiles on the lower surface of an existing, stainless steel orbiter model were as follows:

1) Tile pattern—A symmetric herringbone tile pattern was used.

2) Tile area of interest—The tile pattern begins 2% length aft of the nose, covering the lower area up to the tangent line of the chines and wing leading edge, and extending rearward to 80% length of the model.

3) Selection of tiles to be "raised"—Tiles were randomly selected to provide 25% raised tiles in area of interest. The tile pattern is symmetrical about the centerline (instrumentation is located on and to one side of centerline).

4) Tile size—Selected tiles were plated to 0.0010-in. height. Tiles formed by electrochemical etching had a height of 0.002 in. The tiles were 0.105 in. square.

A resist photographic method was used to mask the model surface except for exposure of the tiles selected for plating or etching. The tile pattern was generated by first accurately drawing all of the lower tiles with a computer-driven drafting machine. A table of random numbers was used to designate which 25% of the tiles would be raised and these were covered with black tape. The drawing was then used to provide a 0.0175-scale negative and positive of the selected tile pattern.

The electroless plating process is described in Ref. 2. The plated model is shown in Fig. 1. After completing the wind-tunnel tests with the plated-tile model, the plating was removed and 75% of the steel surface area was removed by electrochemical means to a depth of 0.002 in. The other 25%

of the model surface was masked with resist. The "islands" thus formed on the steel surface simulated a tile pattern that was identical to the plated model.

Wind-Tunnel Test Program

The 0.0175-scale orbiter model chosen for this experiment had been previously tested in a smooth-surface condition at the Air Force Arnold Engineering Development Center (AEDC) Tunnel B³ and Tunnel F.⁴ These tests provided the base data for three subsequent test programs⁵⁻⁷ conducted to assess the influence of the tile roughness on heat-transfer and boundary-layer transition for this configuration. The discussion on test results will be limited in scope to primarily illustrate the application of the newly developed electroless plating and electrochemical etching techniques to surface-roughness-induced boundary-layer transition studies. Only Tunnel B data will be used to illustrate this model application and data behavior. Detailed analysis and correlation of these test data are presented in a separate publication.⁸

Mach 8 heat-transfer data from three different test programs conducted in AEDC Tunnel B^{3,5,7} were obtained for angles-of-attack ranging 25-40 deg, and freestream Reynolds numbers of $0.5-3.75 \times 10^6$ per ft. Wall-to-total temperature ratios (T_w/T_f) varied 0.42-0.12 for all three test programs. The same basic model and heat-transfer instrumentation (i.e., coaxial surface thermocouple gauges) were also used for all three test programs. However, the surface roughness characteristics were changed for each test. During the first test,³ designated OH-4A, the model had an aerodynamically smooth surface, while in the later two tests, MH-2A⁵ and MH-2B⁷, the model had surface roughness elements representing full scale mismatches of adjacent tile heights of 0.057-in. and 0.114-in., respectively. These two different tile roughness heights were applied over the same tile pattern using selective electroless plating for the 0.057-in. mismatch and selective electrochemical etching to form the 0.114-inch mismatch. Results of these tests will be shown for only the highest Reynolds number tested and two wall temperatures, since these data dramatically illustrate the effects of both roughness and surface cooling on boundary-layer transition for this orbiter configuration.

The effects of both roughness and cooling on the location of boundary-layer transition for the orbiter at Mach 8, $Re/ft = 3.75 \times 10^6$, and 30-deg angle of attack are illustrated in Fig. 2. This figure shows the normalized heat-transfer distributions (normalized to the heating rate at the stagnation point of a scaled 1-ft radius sphere in the same freestream test

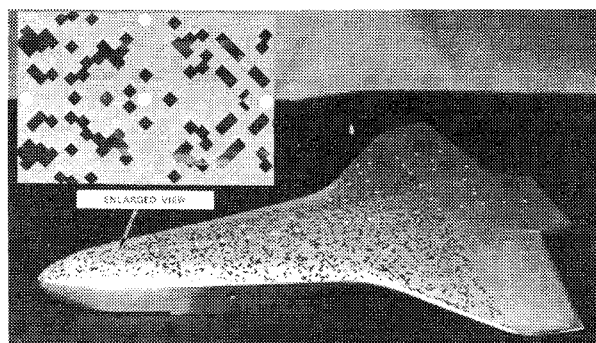


Fig. 1 0.0175-scale orbiter model with 25% tiles plated to 0.001-in. height.

Received May 13, 1977.

Index categories: Testing, Flight and Ground; Boundary Layers and Convective Heat Transfer—Laminar; Boundary Layers and Convective Heat Transfer—Turbulent.

*Senior Engineer. Member AIAA.

†Senior Engineer. Member AIAA.

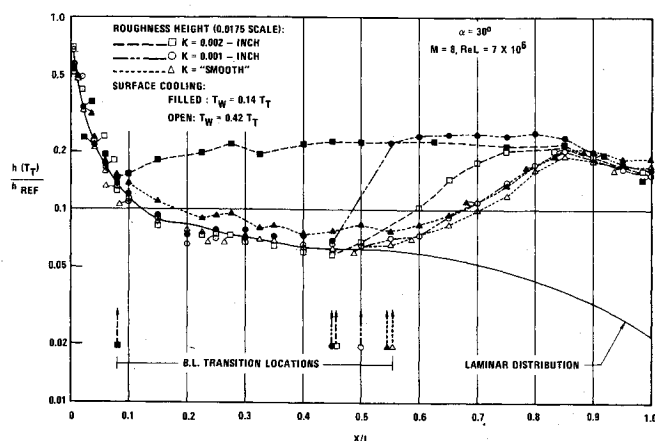


Fig. 2 Orbiter centerline heat-transfer distribution illustrating the influence of surface roughness and cooling on boundary-layer transition.

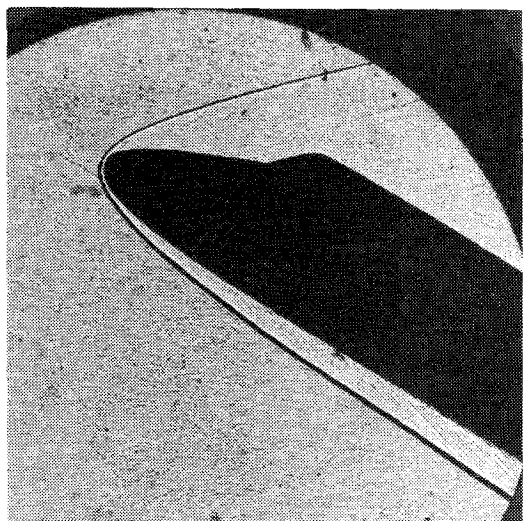


Fig. 3 Shadowgraph of shock layer for orbiter with simulation of tile roughness on lower surface, $M=8$, $Re/ft = 3.7 \times 10^6$, $\alpha=30$ deg, $T_w/T_T=0.42$.

conditions) along the windward surface centerline for all three test programs. A laminar heating distribution is also shown for reference. The data in Fig. 2 indicate that the surface-roughness elements considered herein did not significantly alter the orbiter boundary-layer transition location for $T_w=0.42 T_T$. When the model was cooled to $T_w=0.14 T_T$, the locations of boundary-layer transition did not move significantly for either the smooth-surface test (OH-4A) or the intermediate-surface-roughness test (MH-2A, full-scale roughness elements of 0.057 in.). However, at the cold wall temperature ($T_w=0.14 T_T$), the location of boundary-layer transition moved significantly forward (from approximately 0.45L to 0.08L) for the MH-2B test which represented full scale roughness elements of 0.114 in. Flowfield and boundary-layer analyses⁸ are underway to better understand and correlate this phenomena for use at the orbiter flight conditions.

Additional information concerning the effect of these simulated heat-shield tiles on the orbiter windward shock layer was observed from shadowgraphs (Figs. 3 and 4). These figures show qualitative flowfield data (density perturbations) in the shock layer from tests of a "rough" (0.001-in. tile height) and a "smooth" surface orbiter configuration at the same test conditions ($\alpha=30$ deg, $M=8$, $Re/ft = 3.7 \times 10^6$, $T_w/T_T=0.42$). Examination of these shadowgraphs revealed that the "rough" configuration (Fig. 3) "disturbed" (in a qualitative sense) the shock layer more than the "smooth"

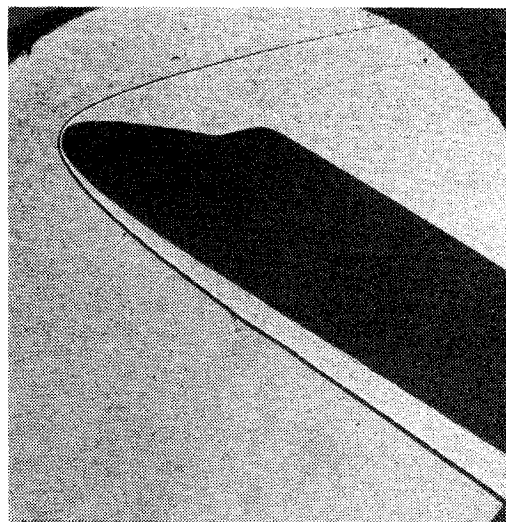


Fig. 4 Shadowgraph of shock layer for orbiter with smooth surface, $M=8$, $Re/ft = 3.7 \times 10^6$, $\alpha=30$ deg, $T_w/T_T=0.42$.

configuration (Fig. 4). This disturbance was apparently restricted to perturbing the shock layer, since few noticeable changes in the measured surface heating rates occurred for these test conditions (Fig. 2). Changes in wall temperature produced small but discernible differences in the perturbations observed from the shadowgraphs. The coaxial heating gage employed in this model did not provide comparisons of surface fluctuations, "noise" or differences in the "localized" heating between the two test configurations.

Concluding Remarks

Preliminary data from heat-transfer tests obtained using an orbiter configuration with various degrees of roughness indicate that, in general, surface roughness elements (representing misaligned, geometrically scaled heatshield tiles) play a minor role in promoting boundary-layer transition at $T_w=0.42 T_T$ (typical of wind-tunnel test conditions). However, dramatic changes in the locations of boundary-layer transition may occur upon cooling the orbiter surface to $0.14 T_T$ (a value typifying hypersonic flight conditions). That is, for roughness elements smaller than 0.001 in. (0.057 in. full scale), the location of boundary-layer transition remains essentially unchanged from aerodynamically smooth locations, whereas for full-scale roughness elements 0.114 in. high, transition moves significantly forward (i.e., from 0.45L to 0.08L). These results may significantly influence the manufacturing tolerances currently being imposed on the orbiter heatshield development program.

Acknowledgment

The application reported herein and other aeroheating model developments featuring electroless plating^{1,2} were supported by NASA-Johnson Space Center under Contract NAS9-13692 to Vought Corporation and test arrangements with AF AEDC and NASA ARC.

References

- ¹Stalmach, C.J. and Goodrich, W.D., "Aeroheating Model Advancements Featuring Electroless Metallic Plating," *Journal of Spacecraft and Rockets*, Vol. 14, Oct. 1977, pp. 600-605.
- ²Stalmach, C.J., "Developments in Convective Heat Transfer Models Featuring Seamless and Selected-Detail Surfaces, Employing Electroless Plating," Vought Corporation, TR2-57110/5R-3227, June 1975; also NASA CR 144364.
- ³Martindale, W.R. and Trimmer, L.L., "Test Results from the NASA/Rockwell International Space Shuttle Test (OH-4A) Conducted in the AEDC-VKF Tunnel B.," AEDC-DR-74-39, May 1974.
- ⁴Boudreau, A.H., "Test Results from the NASA/RI Shuttle Heating Test OH-11 in the AEDC-VKF Tunnel F.," AEDC-DR-74-16, Feb. 1974.

⁵Siler, L.G. and Martindale, W.R., "Test Results from the NASA Space Shuttle Orbiter Heating Test (MH-2) Conducted in the AEDC-VKF Tunnel, B," AEDC-DR-75-103, Oct. 1975.

⁶Siler, L.G., "Test Results from the NASA Space Shuttle Orbiter Heating Test (MH-1) Conducted in the AEDC-VKF Tunnel F," AEDC-DR-76-13, May 1976.

⁷Wannenwetsch, G.D. and Martindale, W.R., "Roughness and Wall Temperature Effects on Boundary-Layer Transition on a 0.0175 Scale Space Shuttle Orbiter Model Tested at Mach Number 8," AEDC-TR-77-19, April 1977.

⁸Bertin, J.J., Idar, E.S., and Goodrich, W.D., "Effect of Surface Cooling and Roughness on Transition for the Shuttle Orbiter," AIAA Paper 77-704, June 1977.

Satellite Attitude Determination by Simultaneous Line-of-Sight Sightings

Carl Grubin*

Northrop Corporation, Hawthorne, Calif.

SUPPOSE that a satellite carries two onboard angle trackers that can make simultaneous measurements of the lines-of-sight to two known references, e.g., two stars, or one star and one Earth-landmark. Then the vehicle attitude at the instant of the sightings can be determined as a linear combination of unit vectors along the lines of sight and their cross product, where the coefficients are functions of the azimuth and elevation of the angle trackers.

Analysis

Let L_1, L_2 be unit vectors along the known lines-of-sight. These ultimately are to be expressed in components in some inertial reference frame. Suppose that L_1, L_2 also are measured in the vehicle frame in terms of azimuth and elevation of the angle-tracking devices. Let i, j, k be unit vectors along the vehicle axes. Then

$$L_i = ia_{i1} + ja_{i2} + ka_{i3} \quad (i=1,2) \quad (1)$$

Received June 8, 1977.

Index categories: Spacecraft Dynamics and Control; Spacecraft Navigation, Guidance, and Flight-Path Control.

*Engineering Specialist, Electronics Division. Associate Fellow AIAA.

where

$$a_{i1} = \cos E_i \cos A_i \quad a_{i2} = \cos E_i \sin A_i \quad a_{i3} = \sin E_i$$

Since L_1, L_2 are not parallel, a third independent equation can be constructed from Eqs. (1) by forming the cross-product. Combining the cross-product equation with the original equations produces

$$M \begin{bmatrix} i \\ j \\ k \end{bmatrix} = \begin{bmatrix} L_1 \\ L_2 \\ L_1 \times L_2 \end{bmatrix} \quad (2)$$

where

$$M = \begin{bmatrix} a_{11} & a_{12} & a_{13} \\ a_{21} & a_{22} & a_{23} \\ (a_{12}a_{23} - a_{13}a_{22}) & (a_{13}a_{21} - a_{11}a_{23}) & (a_{11}a_{22} - a_{12}a_{21}) \end{bmatrix}$$

Solving Eqs. (2)

$$\begin{bmatrix} i \\ j \\ k \end{bmatrix} = M^{-1} \begin{bmatrix} L_1 \\ L_2 \\ L_1 \times L_2 \end{bmatrix} \quad (3)$$

Thus i, j, k are expressible as linear combinations of L_1, L_2 , and $L_1 \times L_2$. Geometrically, sighting L_1 places the vehicle axes i, j, k somewhere on three individual cones whose common axis is L_1 and whose semivertex angles are $\cos^{-1}(a_{11}), \cos^{-1}(a_{12}), \cos^{-1}(a_{13})$, respectively. Similarly, sighting L_2 places i, j, k somewhere on three other cones whose common axis is L_2 and whose semivertex angles are $\cos^{-1}(a_{21}), \cos^{-1}(a_{22}), \cos^{-1}(a_{23})$. According to Ref. 1, there are, in general, two solutions for each of i, j, k , or eight sets of solutions altogether. The solution produced by Eq. (3) is the unique correct solution in that it enjoys the property that i, j, k is an orthogonal set satisfying the right-hand rule.

References

- Grubin, C., "A Simple Algorithm for Intersecting Two Conical Surfaces," *Journal of Spacecraft and Rockets*, Vol. 14, April 1977, pp. 251-252.